

Palladium-Catalyzed C–H Functionalization of Acyldiazomethane and Tandem Cross-Coupling Reactions

Fei Ye,^{†,||} Shuanglin Qu,^{‡,||} Lei Zhou,^{§,||} Cheng Peng,[†] Chengpeng Wang,[†] Jiajia Cheng,[†] Mohammad Lokman Hossain,[†] Yizhou Liu,[†] Yan Zhang,[†] Zhi-Xiang Wang,^{*,‡} and Jianbo Wang^{*,†}

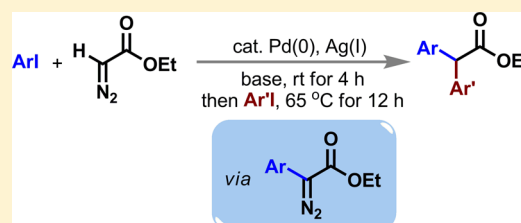
[†]Beijing National Laboratory of Molecular Sciences, Key Laboratory of Bioorganic Chemistry and Molecular Engineering of Ministry of Education, College of Chemistry, Peking University, Beijing 100871 China

[‡]School of Chemistry and Chemical Engineering, University of Chinese Academy of Sciences, Beijing 100049, China

[§]School of Chemistry and Chemical Engineering, Sun Yat-Sen University, Guangzhou 510275, China

Supporting Information

ABSTRACT: Palladium-catalyzed C–H functionalization of acyldiazomethanes with aryl iodides has been developed. This reaction is featured by the retention of the diazo functionality in the transformation, thus constituting a novel method for the introduction of diazo functionality to organic molecules. Consistent with the experimental results, the density functional theory (DFT) calculation indicates that the formation of Pd–carbene species in the catalytic cycle through dinitrogen extrusion from the palladium ethyl diazoacetate (Pd–EDA) complex is less favorable. The reaction instead proceeds through Ag₂CO₃ assisted deprotonation and subsequently reductive elimination to afford the products with diazo functionality remained. This C–H functionalization transformation can be further combined with the recently evolved palladium-catalyzed cross-coupling reaction of diazo compounds with aryl iodides to develop a tandem coupling process for the synthesis of α,α -diaryl esters. DFT calculation supports the involvement of Pd–carbene as reactive intermediate in the catalytic cycle, which goes through facile carbene migratory insertion with a low energy barrier (3.8 kcal/mol).



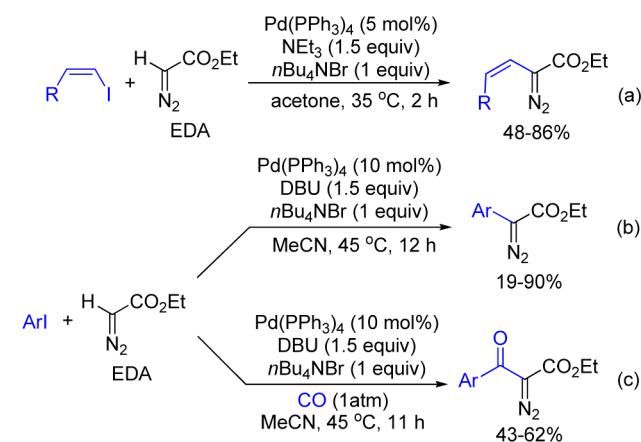
INTRODUCTION

Diazo compounds are commonly used as metal carbene precursors in transition-metal-catalyzed reactions. In general, diazo compounds are highly reactive substrates in transition metal catalysis. In most cases transition-metal-catalyzed dediazonation occurs readily to generate short-lived metal carbene species, which undergoes a wide array of metal carbene transformations, such as C–H insertions, X–H insertions (X = O, N, S, Si, etc.), cyclopropanations, and ylide formations. These reactions have found wide applications in organic synthesis.¹

In 2007, we developed a palladium-catalyzed reaction of ethyl diazoacetate (EDA) with aryl or vinyl iodides (Scheme 1).² Subsequently, the groups of Frantz and Reissig reported similar coupling reactions.³ A surprising feature of this type of coupling reactions is that the diazo moiety retains in the products, and thus, the transformation can be viewed as a C–H functionalization of EDA.⁴ Moreover, when the reaction is carried out under an atmosphere of CO, carbonylation occurs to afford β -keto- α -diazoesters (Scheme 1c).²

This coupling reaction, which seems to be the first example of transition-metal-catalyzed C–H functionalization of EDA, provides a potentially useful approach to introduce diazo functionality to organic compounds.^{5,6} However, the reaction is not efficient with relatively low yields and limited scope. In particular, the vinyl iodides are limited to those bearing

Scheme 1. Palladium-Catalyzed Cross-Coupling of EDA



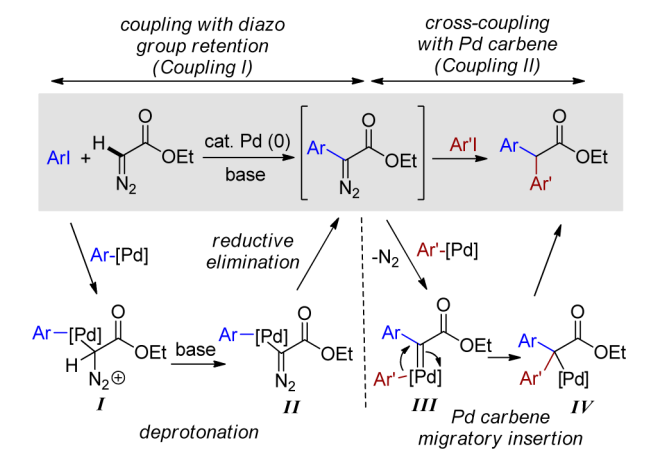
electron-withdrawing groups (Scheme 1a, R = ester or ketone), while the diazo substrate is only limited to EDA. Therefore, it is essential to further optimize the reaction conditions in order to make this transformation a practical method for the synthesis of diazo compounds.

Received: December 31, 2014

Published: March 20, 2015

Furthermore, diazo compounds have recently emerged as a new type of partners in palladium-catalyzed cross-coupling reactions. Pd–carbene species are suggested to be the key intermediates undergoing migratory insertions to form C–C bond.⁷ This type of coupling reaction has been shown to be general, with the migratory group being aryl, benzyl, allyl, allenyl, alkynyl, acyl, and vinyl group.^{7,8} Notably, for the palladium-catalyzed C–H functionalization of EDA with aryl or vinyl iodides (Scheme 2, coupling I), the reaction temperature

Scheme 2. Palladium-Catalyzed Tandem Cross-Coupling with EDA



is slightly lower as compared with the palladium-catalyzed cross-coupling reactions involving carbene intermediates (Scheme 2, coupling II). We conceived that with the same Pd catalyst a tandem coupling reactions may be possible, thus generating two different C–C bonds on the carbon that bears diazo functionality of the diazo substrate. Herein we wish to report an efficient three-component coupling reaction of ArI, Ar'I, and EDA via palladium-catalyzed coupling (C–H functionalization)/migratory insertion sequence.

The tandem coupling (Scheme 2) also raises intriguing mechanistic issues. Of particular interest, in the palladium-catalyzed C–H functionalization of EDA with aryl or vinyl iodides (coupling I), the Pd–carbene is obviously not generated from intermediate I; thus, the products with diazo moiety remaining intact could be produced. However, in the subsequent palladium-catalyzed coupling of aryl diazoacetate with aryl iodide (coupling II), the Pd–carbene III should be formed, thus leading to the final products via migratory insertion according to previous studies.^{7,8} To gain insights into the details of these processes, DFT (density functional theory) mechanistic computations were carried out for both coupling stages. The computations indicate that the dediazonation to form Pd–carbene from the palladium–EDA complex I is energetically less competitive with the C–H activation generating II despite being feasible, and support the involvement of Pd–carbene III as reactive intermediate in the palladium-catalyzed coupling of aryl diazoacetate with aryl iodide, followed by a facile migratory insertion to form palladium species IV with an energy barrier as low as 3.8 kcal/mol.

RESULTS AND DISCUSSION

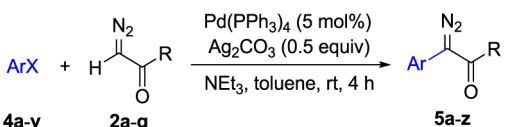
Reaction Optimization and Scope. Our initial catalysts screening revealed Pd(PPh₃)₄ to be the most active catalyst for

Table 1. Palladium-Catalyzed Cross-Coupling of Vinyl Halides with EDA^a

entry	vinyl halide	product	yield% ^b
1			95
2			91
3			90
4			72
5			73
6			67
7			72
8			82
9			72
10			49
11			54
12			77
13			66

^aReaction conditions: aryl halides (0.5 mmol), EDA (1.3 equiv), NEt₃ (1.3 equiv), Ag₂CO₃ (0.5 equiv), Pd(PPh₃)₄ (5 mol %), in 2 mL of toluene at room temperature for 4 h. ^bIsolated yield by column chromatography with silica gel.

cross-coupling of (*Z*)-ethyl 3-iodoacrylate **1a** and EDA **2a**, whereas other palladium catalysts were found to decompose the diazo compound rapidly to give a complex mixture. The introduction of 1 equiv of *n*-Bu₄NBr as additive could appreciably improve the yield of the coupling product **3a**. It was also found that the reaction gave better results in the polar solvent and with NEt₃ as the base. We then concentrated our

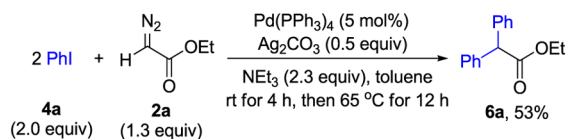
Table 2. Palladium-Catalyzed Cross-Coupling of Aryl Halides with Diazo Compounds 2a–g^a


entry	4, ArX	2, R =	5, yield (%) ^b
1	4a, C ₆ H ₅ I	2a, OEt	5a, 86
2	4b, <i>p</i> -MeC ₆ H ₄ I	2a, OEt	5b, 82
3	4c, <i>m</i> -MeC ₆ H ₄ I	2a, OEt	5c, 84
4	4d, <i>p</i> -MeOC ₆ H ₄ I	2a, OEt	5d, 86
5	4e, <i>p</i> -ClC ₆ H ₄ I	2a, OEt	5e, 83
6	4f, <i>p</i> -MeO ₂ CC ₆ H ₄ I	2a, OEt	5f, 91
7	4g, <i>p</i> -NO ₂ C ₆ H ₄ I	2a, OEt	5g, 96
8	4h, <i>p</i> -BrC ₆ H ₄ I	2a, OEt	5h, 86
9	4i, <i>p</i> -F ₃ CC ₆ H ₄ I	2a, OEt	5i, 92
10	4j, <i>p</i> -NCC ₆ H ₄ I	2a, OEt	5j, 81
11	4k, <i>m</i> -FC ₆ H ₄ I	2a, OEt	5k, 84
12	4l, <i>p</i> -HOH ₂ CC ₆ H ₄ I	2a, OEt	5l, 89
13	4m, <i>m</i> -H ₂ NC ₆ H ₄ I	2a, OEt	5m, 55
14	4n, 4-iodopyridine	2a, OEt	5n, 95
15	4o, 1-iodonaphthalene	2a, OEt	5o, 38
16	4p, 3-iodothiophene	2a, OEt	5p, 22
17	4q, <i>p</i> -O ₂ NC ₆ H ₄ I	2b, Ph	5q, 90
18	4g, <i>p</i> -O ₂ NC ₆ H ₄ I	2c, Me	5r, 99
19	4f, <i>p</i> -MeO ₂ CC ₆ H ₄ I	2b, Ph	5u, 80
20	4q, <i>p</i> -PhC ₆ H ₄ I	2b, Ph	5v, 47
21	4a, C ₆ H ₅ I	2d, CH ₂ Ph	5w, 78
22	4a, C ₆ H ₅ I	2e, 2,6-di- <i>t</i> Bu-4-MeC ₆ H ₃	5x, 97
23	4g, <i>p</i> -O ₂ NC ₆ H ₄ I	2f, NPh ₂	5s, 81
24	4g, <i>p</i> -O ₂ NC ₆ H ₄ I	2g, N(<i>i</i> -Pr) ₂	5t, 77
25	4r, <i>p</i> -O ₂ NC ₆ H ₄ Br	2a, OEt	5g, 70
26	4s, <i>p</i> -NCC ₆ H ₄ Br	2a, OEt	5j, 63
27	4t, <i>p</i> -F ₃ CC ₆ H ₄ Br	2a, OEt	5i, 30
28	4u, 3,5-di-F ₃ CC ₆ H ₃ Br	2a, OEt	5y, 40
29	4v, 3,5-di-BrC ₆ H ₃ Br	2a, OEt	5z, 34

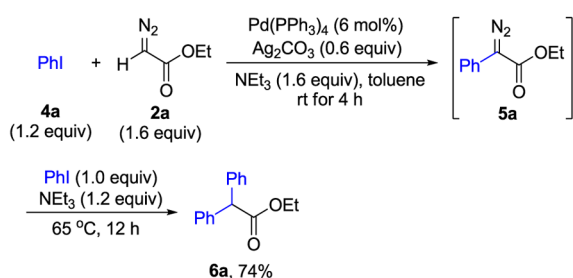
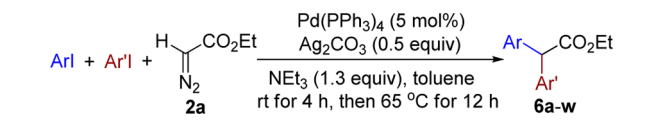
^aAll the reactions were carried out with aryl iodides 4a–v (0.5 mmol), 2a–g (1.3 equiv), NEt₃ (1.3 equiv), Ag₂CO₃ (0.5 equiv) in the presence of Pd(PPh₃)₄ (5 mol %) in toluene at room temperature for 4 h. ^bIsolated yield by column chromatography with silica gel.

Scheme 3. Tandem Cross-Coupling Reaction

A) one-step addition of 4a



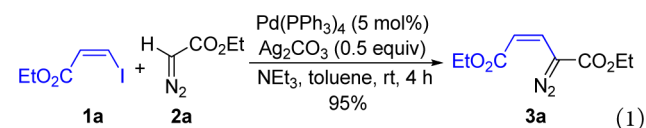
B) stepwise addition of 4a

Table 3. Palladium-Catalyzed Tandem Cross-Coupling of Aryl Iodides, Aryl Iodides, and EDA^a


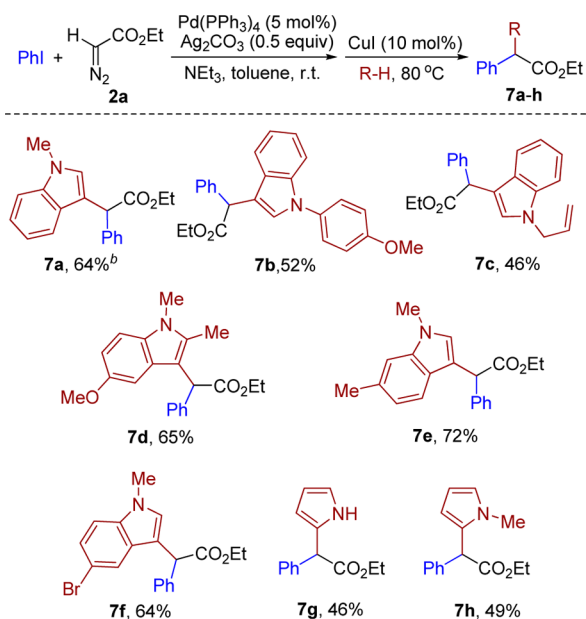
entry	ArI	Ar'I	Ar'I	6, yield (%) ^b
1	4a, C ₆ H ₅ I	4a, C ₆ H ₅ I	4a, C ₆ H ₅ I	6a, 74
2	4b, <i>p</i> -MeC ₆ H ₄ I	4b, <i>p</i> -MeC ₆ H ₄ I	4b, <i>p</i> -MeC ₆ H ₄ I	6b, 77
3	4c, <i>m</i> -MeC ₆ H ₄ I	4c, <i>m</i> -MeC ₆ H ₄ I	4c, <i>m</i> -MeC ₆ H ₄ I	6c, 71
4	4w, <i>o</i> -MeOC ₆ H ₄ I	4w, <i>o</i> -MeOC ₆ H ₄ I	4w, <i>o</i> -MeOC ₆ H ₄ I	6w, trace
5	4d, <i>p</i> -MeOC ₆ H ₄ I	4d, <i>p</i> -MeOC ₆ H ₄ I	4d, <i>p</i> -MeOC ₆ H ₄ I	6d, 73
6	4x, <i>m</i> -MeOC ₆ H ₄ I	4x, <i>m</i> -MeOC ₆ H ₄ I	4x, <i>m</i> -MeOC ₆ H ₄ I	6e, 79
7	4e, <i>p</i> -ClC ₆ H ₄ I	4e, <i>p</i> -ClC ₆ H ₄ I	4e, <i>p</i> -ClC ₆ H ₄ I	6f, 71
8	4f, <i>p</i> -MeO ₂ CC ₆ H ₄ I	4f, <i>p</i> -MeO ₂ CC ₆ H ₄ I	4f, <i>p</i> -MeO ₂ CC ₆ H ₄ I	6g, 75
9	4q, <i>p</i> -PhC ₆ H ₄ I	4q, <i>p</i> -PhC ₆ H ₄ I	4q, <i>p</i> -PhC ₆ H ₄ I	6h, 66
10	4a, C ₆ H ₅ I	4d, <i>p</i> -MeOC ₆ H ₄ I	4a, C ₆ H ₅ I	6i, 66
11	4d, <i>p</i> -MeOC ₆ H ₄ I	4a, C ₆ H ₅ I	4a, C ₆ H ₅ I	6i, 64
12	4f, <i>p</i> -MeO ₂ CC ₆ H ₄ I	4a, C ₆ H ₅ I	4a, C ₆ H ₅ I	6j, 70
13	4f, <i>p</i> -MeO ₂ CC ₆ H ₄ I	4b, <i>p</i> -MeC ₆ H ₄ I	4b, <i>p</i> -MeC ₆ H ₄ I	6k, 73
14	4f, <i>p</i> -MeO ₂ CC ₆ H ₄ I	4y, <i>m,p</i> -Me ₂ C ₆ H ₃ I	4y, <i>m,p</i> -Me ₂ C ₆ H ₃ I	6l, 67
15	4f, <i>p</i> -MeO ₂ CC ₆ H ₄ I	4d, <i>p</i> -MeOC ₆ H ₄ I	4d, <i>p</i> -MeOC ₆ H ₄ I	6m, 65
16	4q, <i>p</i> -PhC ₆ H ₄ I	4a, C ₆ H ₅ I	4a, C ₆ H ₅ I	6n, 71
17	4d, <i>p</i> -MeOC ₆ H ₄ I	4q, <i>p</i> -PhC ₆ H ₄ I	4q, <i>p</i> -PhC ₆ H ₄ I	6o, 63
18	4a, C ₆ H ₅ I	4g, <i>p</i> -O ₂ NC ₆ H ₄ I	4g, <i>p</i> -O ₂ NC ₆ H ₄ I	6p, 64
19	4a, C ₆ H ₅ I	4j, <i>p</i> -NCC ₆ H ₄ I	4j, <i>p</i> -NCC ₆ H ₄ I	6q, 54
20	4a, C ₆ H ₅ I	4o, 1-iodonaphthalene	4o, 1-iodonaphthalene	6r, 51
21	4x, <i>m</i> -MeOC ₆ H ₄ I	4y, <i>p</i> -FC ₆ H ₄ I	4y, <i>p</i> -FC ₆ H ₄ I	6s, 56
22	4x, <i>m</i> -MeOC ₆ H ₄ I	4i, <i>p</i> -F ₃ CC ₆ H ₄ I	4i, <i>p</i> -F ₃ CC ₆ H ₄ I	6t, 60
23	4x, <i>m</i> -MeOC ₆ H ₄ I	4z, <i>o</i> -ClC ₆ H ₄ I	4z, <i>o</i> -ClC ₆ H ₄ I	6u, 56
24	4y, <i>p</i> -FC ₆ H ₄ I	4x, <i>m</i> -MeOC ₆ H ₄ I	4x, <i>m</i> -MeOC ₆ H ₄ I	6s, 69

^aReaction conditions: a solution of ArI (0.48 mmol), EDA 2a (0.64 mmol), NEt₃ (0.64 mmol), Ag₂CO₃ (0.24 mmol), and Pd(PPh₃)₄ (0.024 mmol) in toluene (2 mL) was stirred at room temperature for 4 h and then Ar'I (0.4 mmol) and NEt₃ (0.48 mmol) were added; the resulted mixture was heated at 65 °C for another 12 h. ^bIsolated yield with silica gel column chromatography.

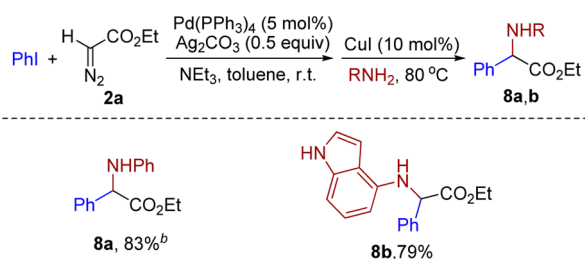
reoptimization efforts on the testing of a series of additives. After some experimentation, we obtained the optimized reaction conditions as the following: 0.5 equiv of Ag₂CO₃ as additive and NEt₃ as base in toluene at room temperature. Under such conditions, the reaction could afford the coupling product 3a in 95% isolated yield (eq 1).



Next we explored the scope of the new catalytic system with various vinyl halides. As shown in Table 1, the cross-coupling of vinyl iodides 1a–e with EDA, which only resulted in moderate yields in our previous report, now proceeds efficiently to afford the corresponding diazo esters in excellent yields (entries 1–5). For example, the yield of 3d was improved from 48% to 72% by using the newly optimized reaction conditions. Besides, a limitation of the previous reaction is that the reaction only works for the substrates with strong electron-withdrawing substituents at the double bond.² Gratifyingly, under the new reaction conditions, β-iodo styrene derivatives could also react with EDA smoothly to give the corresponding products in moderate yields (entries 6–9). Vinyl bromides, which are less

Scheme 4. Palladium-Catalyzed C–H Functionalization of EDA/Copper-Catalyzed Formal R–H Insertion Cascade^a


^aReaction conditions: a solution of PhI (0.48 mmol), EDA 2a (0.64 mmol), NEt₃ (0.64 mmol), Ag₂CO₃ (0.24 mmol), and Pd(PPh₃)₄ (0.024 mmol) in toluene (2 mL) was stirred at room temperature for 4 h and then RH (0.4 mmol), CuI (0.04 mmol) were added. The resulted mixture was heated at 80 °C for 2 h. ^bIsolated yield with silica gel column chromatography.

Scheme 5. Palladium-Catalyzed C–H Functionalization of EDA/Copper-Catalyzed N–H Insertion Cascade^a


^aReaction conditions are same as described in Scheme 4. ^bIsolated yield with silica gel column chromatography.

reactive but more readily available than the corresponding vinyl iodides, were also suitable substrates for the cross-coupling with EDA, leading to the corresponding coupling products in moderate to good yields (entries 10–13). It is noteworthy that in all the cases the cross-coupling reaction proceeded with retention of configuration at the double bond.

In our previous report, the reaction conditions for the coupling of vinyl iodides with EDA were not efficient when vinyl iodides were extended to the aryl iodides. Although the palladium-catalyzed cross-coupling of aryl iodides with EDA was realized upon modified reaction conditions, the generality and efficiency of the reaction were still limited.² Encouraged by the improved yields for the coupling of vinyl halides and EDA, we applied the new catalytic conditions to the cross-coupling reaction of aryl iodides with EDA. We were pleased to find that various aryl iodides reacted smoothly with EDA in the presence of 5 mol % of Pd(PPh₃)₄ and 0.5 equiv of Ag₂CO₃. The reaction carried out in toluene at room temperature for 4 h

afforded the corresponding products in good to excellent yields (Table 2). Compared with the previous results, the present reaction conditions afforded better yields with lower catalyst loading, and the reaction completed within shorter time at room temperature and showed much wider substrate scope. As shown in Table 2, aryl iodides bearing electron-donating (entries 2–4) or electron-withdrawing (entries 5–11) groups all worked well under the identical conditions. To our delight, free –OH and –NH₂ also tolerated this transformation (entries 12 and 13). Besides, the diazo product bearing pyridine, thiophene, and naphthalene were obtained under the same conditions (entries 14–16). The substrate scope was then expanded to diazoketones.

It was found that a series of functional groups were survived under the optimized reaction conditions to afford the corresponding products (entries 17–22). Similarly, phenyl-diazoamides were obtained successfully via this transformation (entries 23 and 24).

Finally, the cross-coupling between aryl bromides with ethyl diazoacetate 2a was examined. It was found that aryl bromides could also give the corresponding products under the conditions, albeit in lower yields (entries 25–29).

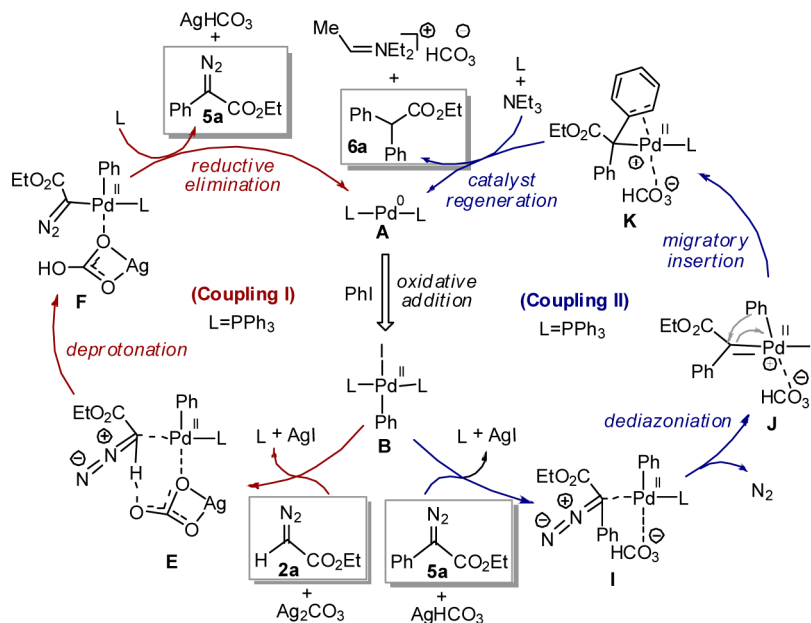
Since palladium catalysts also catalyze the cross-coupling reaction of the aryldiazoacetates such as 5a–z with aryl halides,^{7,8} we thus considered the possibility to carry out further coupling reaction in the same reaction system with the same palladium catalyst upon the completion of the coupling of aryl iodides and acyldiazomethanes. Such a tandem process, in which multiple chemical transformations are performed with single catalyst sequentially in a single reaction vessel without intermediary purification steps, should significantly increase the efficiency of the catalyst and reduce the time, costs, and waste generation.⁹

With this in mind, we initially carried out the reaction in one-pot manner with 1.3 equiv of EDA 2a and 2.0 equiv of iodobenzene 4a in the presence of 5 mol % of Pd(PPh₃)₄, 2.3 equiv of NEt₃, and 0.5 equiv of Ag₂CO₃ in toluene. The reaction mixture was stirred at room temperature for 4 h and then it was heated up to 65 °C for 12 h. The desired product 6a could be isolated in 53% yield (Scheme 3A). However, when two different aryl iodides were subjected to the same one-pot reaction, complex mixture was observed due to the competing homocoupling reactions. To avoid such problem, the same reaction was carried out by adding the aryl iodides and NEt₃ separately. Interestingly, even for the coupling with the same iodobenzene 4a, the reaction gave better yield with separate addition approach (Scheme 3B).

Under the same reaction conditions as shown in Scheme 3B, we then examined the generality of this reaction by employing a variety of aryl iodides to couple with EDA. First, we studied the tandem coupling reactions with same aryl iodides for both steps. As shown in Table 3, aryl iodides with same para or meta substituents all worked well in the present reaction system (entries 1–3). However, only trace of the desired product was detected when ortho-substituted aryl iodide was employed as the substrate in the first step (entry 4). Functional groups, such as chloro, ester, and phenyl, tolerate the reaction conditions, giving the corresponding products in moderate to good yields (entries 5–9).

Next, we proceeded to expand the reaction to the coupling with two different aryl iodides. As shown by the results summarized in Table 3, the coupling reactions all afforded the desired products in comparable yields (entries 10–24). The

Scheme 6. Proposed Catalytic Cycle for the Tandem Coupling Reaction



reaction was found not significantly affected by the electronic properties of the substituents on the aromatic rings. Aryl iodides substituted by electron-donating or electron-withdrawing groups in either first or second step worked equally well, affording the three-component cross-coupling products in moderately good yields (entries 10–19, 21–24). Notably, 1-iodonaphthalene is also a suitable substrate for the coupling reaction (entry 20).

Since diverse transformations are possible from the aryldiazoacetate intermediates,¹ it is thus possible to further devise various tandem processes through different combinations. Herein we demonstrate the combination of palladium-catalyzed C–H functionalization of EDA with aryl iodides and the Cu(I)-catalyzed C–H/N–H insertions of the aryldiazoacetate intermediates. Following the established reaction conditions for the formal Cu(I)–carbene C–H insertion,^{10,11} indole derivatives were chosen as the substrates for demonstrating the tandem transformation. As shown in Scheme 4, indoles bearing different protecting groups on nitrogen worked well in the tandem reaction (7a–c). Besides, *N*-methylindoles bearing OMe, Me, and Br substituents were also good substrates (7d–f). When pyrroles were introduced into the tandem reaction, the corresponding products were also obtained, but in low yields (7g–h).

Finally, Cu(I)-catalyzed N–H insertion^{10,12} was combined with the Pd(0)-catalyzed C–H functionalization of EDA. The cascade reaction proceeded smoothly, providing the expected products in good yields (Scheme 5).

Computational Studies. To gain insights into the reaction mechanism, we performed DFT mechanistic study using Gaussian 09.^{13,14} We chose the reaction shown in Scheme 3A as a representative for mechanistic investigation.

On the basis of our computational study, Scheme 6 outlines our proposed mechanism for the whole tandem reaction. It is composed of two sequential coupling stages to form two new C–C bonds, namely, coupling I and coupling II. Both stages start with an oxidative addition step of PhI to the Pd(0) catalyst (A). In coupling I, the diazo substrate 2a is deprotonated by Ag₂CO₃ from E to F, followed by C–C coupling via reductive

elimination, giving 5a and regenerating the Pd(0) catalyst A. In coupling II, the diazo intermediate 5a generated in coupling I decomposes by extrusion of N₂ gas from I, resulting in a Pd(II)–carbene species J, then the phenyl group migrates to the Pd(II)–carbene carbon, leading to K with another C–C bond formed. Finally, NEt₃ reduces the Pd(II) complex K back to the Pd(0) catalyst (A) and simultaneously releases the final product 6a, completing the tandem C–C couplings. In the following, we discuss the details of the mechanism in terms of the two stages.

Coupling I. The pathway for coupling I is depicted in Figure 1, together with energetic and key geometric results. This stage can be characterized by three steps, including the oxidative addition of PhI to the Pd(0) catalyst, deprotonation of the diazo substrate 2a by Ag₂CO₃, and reductive elimination to give 5a and regenerate the Pd(0) catalyst simultaneously.

Like many palladium-catalyzed cross-coupling reactions,¹⁵ the catalytic cycle starts from the oxidative addition of PhI to PdL₂ (A). Generally, the oxidative addition gives a *cis* isomer first, but the *cis* isomer can easily isomerize to the more stable *trans* isomer.¹⁶ The mechanism of oxidative addition of aryl halides to Pd(0) species has been well-studied;^{15–17} thus, we did not pursue the details of the process and chose the more stable *trans* isomer (B) to continue the coupling stage. After oxidative addition, one phosphine ligand in B is replaced by Ag₂CO₃, leading to complex C, in which an O atom of Ag₂CO₃ coordinates to the Pd center and a silver atom forms AgI moiety with the iodine atom. The ligand exchange lowers the energy of the system by 7.7 kcal/mol, mainly due to the driving force of forming a stable AgI moiety. Upon forming C, two scenarios were considered for proceeding the coupling. In the first scenario which could be the case in which the concentration of AgI particles is low, e.g., at the beginning of the reaction, the AgI moiety retains. In the second scenario which could occur when the concentration of AgI particles is relatively high, e.g., at the ending of the reaction, the AgI moiety could be extracted by AgI particles. We found that both scenarios are energetically feasible and follow the same mechanism except for some energetic differences. Herein, we

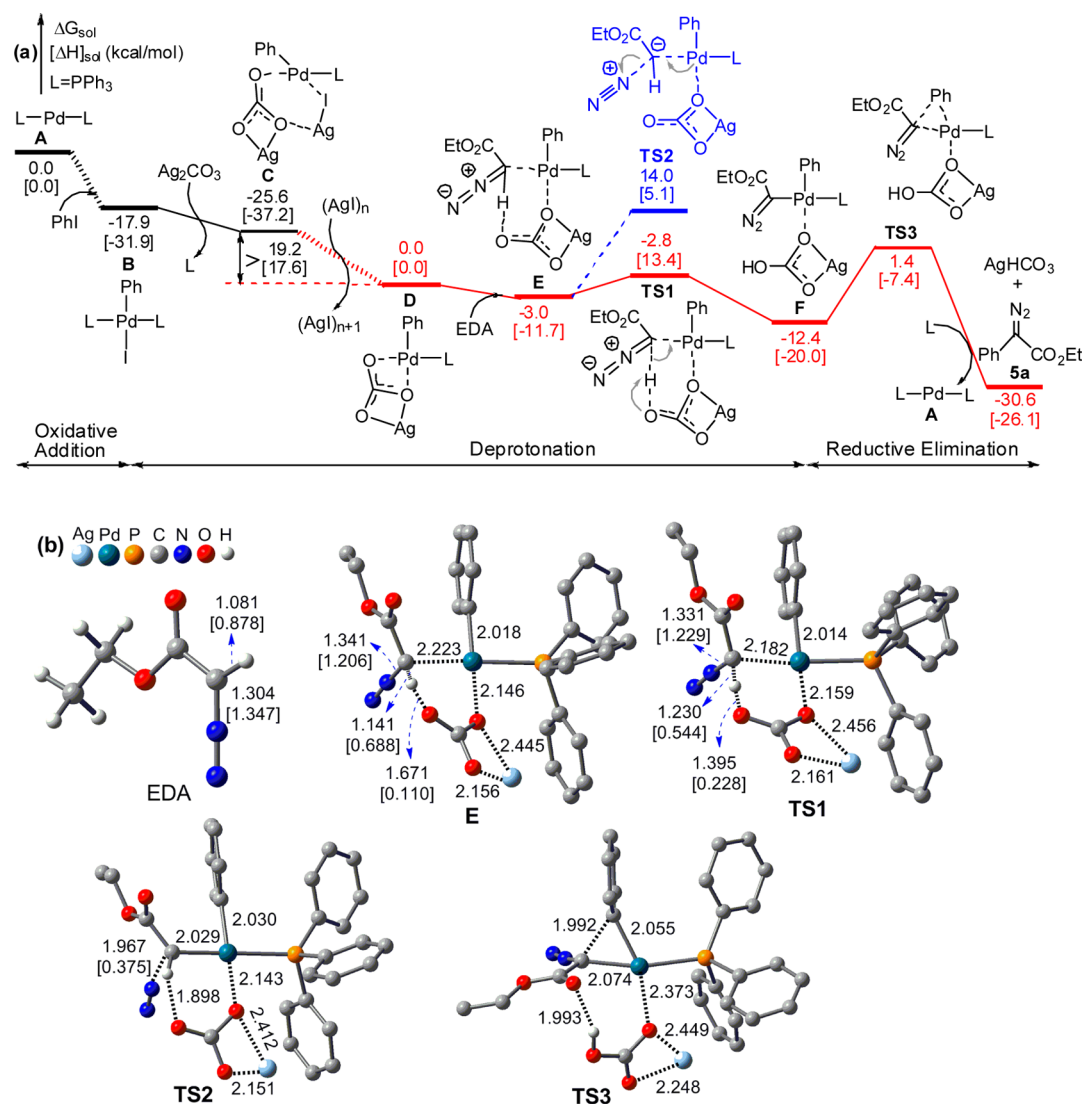


Figure 1. (a) Energy profile of coupling I. (b) Key optimized structures with selected bond lengths in angstroms; the values in brackets are Wiberg bond indices. Trivial hydrogen atoms are omitted for clarity.

continue the discussion based on the results of the second scenario and give the results of the first scenario in Supporting Information (Figure S1). Note that coupling II also features an intermediate (i.e., G in Figure 3) similar to C and we also took both scenarios into account for G to proceed (*vide infra*).

As a simplified model of AgI particles, we used AgI monomer to examine the feasibility of the extraction ($\text{AgI} + \text{C} \rightarrow (\text{AgI})_2 + \text{D}$), which shows that the process is exergonic by 19.2 kcal/mol. Larger AgI particles should drive the extraction more favorably because AgI precipitates. Thus, no matter which size of AgI particle participates in the extraction, the intermediate D can be generated. Considering the uncertainty of the exergonicity of the extraction by different sizes of AgI particles, we select D as energy reference to discuss the process from D to 5a (the red section in Figure 1).

The extraction of AgI from C results in D in which two O atoms of Ag_2CO_3 moiety coordinate to the Pd center. Because EDA features a carbon center bearing a formal lone pair, EDA would attack the Pd center of D, which repels the neighboring (Pd–O) atom, resulting in E in which the repelled O atom forms a C–H...O hydrogen bond with the EDA moiety (see the structure of E in Figure 1b). This process is slightly

exergonic by 3.0 kcal/mol. Once E is formed, the O atom in the C–H...O hydrogen bond grabs the proton of the EDA moiety readily with a barrier of only 0.2 kcal/mol, resulting in F with a AgHCO_3 moiety formed. The facile deprotonation can be attributed to the weakened C–H bond and the proximity of the basic O center. Relative to EDA, the C–H bond in E is stretched by 0.06 Å and the Wiberg bond order¹⁸ of the bond is decreased by 0.19. Finally, the reductive elimination occurs by crossing a barrier of 13.8 kcal/mol (TS3), followed by the recoordination of phosphine ligand to the Pd center, releasing the product (5a) of coupling I and AgHCO_3 and regenerating the catalyst PdL_2 (A). In our one-pot experiments, the base (NET_3) was available in the system. We also considered whether NET_3 can perform the deprotonation, but the results show that NET_3 is less effective than Ag_2CO_3 to perform the deprotonation (see Supporting Information, Figure S3).

Previous studies have found that the diazo fragment of diazo compounds could be readily released to form palladium carbene in various palladium-catalyzed coupling reactions.⁷ Intriguingly, the diazo fragment in this coupling stage maintains. Apparently, E is the possible intermediate to release N_2 . Relative to E, the barrier (TS2) for N_2 release is 17.0 kcal/

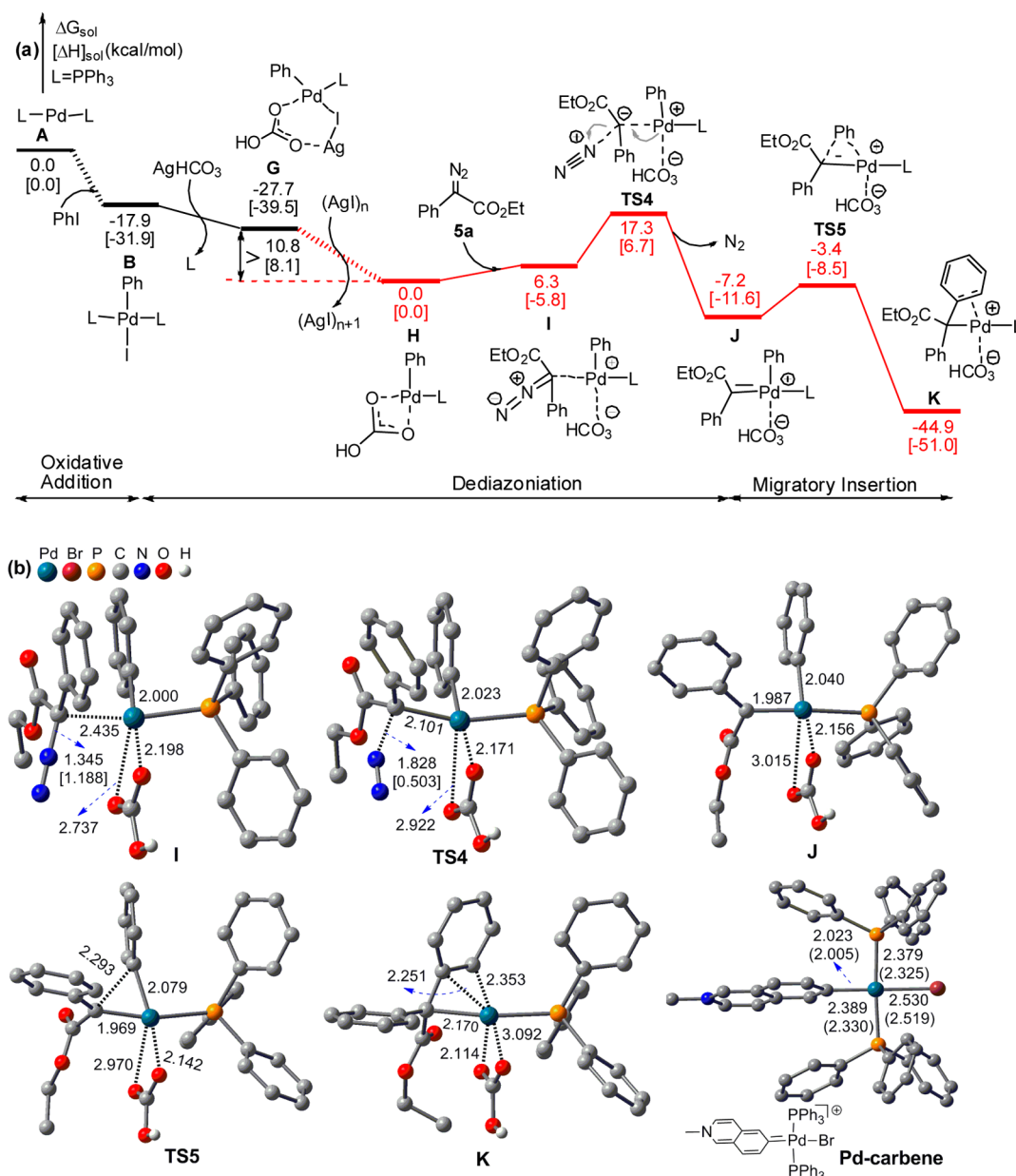


Figure 2. (a) Energy profile for dediazonation and migratory insertion in coupling II. (b) Key optimized structures with selected bond lengths in angstroms; the values in brackets are Wiberg bond indices. Trivial hydrogen atoms are omitted for clarity. The values in parentheses in Pd-carbene are bond lengths in X-ray structure (ref 19e).

mol, which is not high and accessible but is significantly higher than TS1 (by 16.8 kcal/mol). Therefore, the retention of the diazo fragment in this coupling is because the deprotonation is too easy rather than that the N_2 release is so difficult. Note that the EDA coordination in E also weakens the C–N bond, as shown by the elongated bond length by 0.037 Å and decreased bond order by 0.141.

Coupling II. Figures 2 and 3 show the energy profiles of the coupling II stage, together with key structural results. After the oxidative addition from A to B, AgHCO_3 generated in coupling I replaces one of phosphine ligands, giving complex G. Similar to the exergonic process from B to C in Figure 1, the formation of AgI moiety from B to G is also exergonic by 9.8 kcal/mol. G is the counterpart of C. Similarly, G could proceed with AgI either extracted or reserved. The extraction of AgI by AgI monomer from G is exergonic by 10.8 kcal/mol, compared to

19.2 kcal/mol of C. The red section of the energy profile in Figure 2 is for the scenario with AgI removed and that with AgI reserved is given in Supporting Information (Figure S2).

The extraction of AgI from G leads to H. Subsequently, **5a** produced in situ in coupling I attacks the Pd center of H, leading to I. Intermediates H and I correspond to D and E in coupling I, respectively. As the process from D to E is exergonic by 3.0 kcal/mol, the process from H to I is endergonic by 6.3 kcal/mol, which reflects the contribution of the C–H...O hydrogen bond in stabilizing E. In contrast to E, there is no acidic proton in the diazo fragment of I; thus, I can only release N_2 , which needs to climb a barrier of 17.3 kcal/mol (TS4 relative to H + **5a**) and leads to a palladium species J. The barrier is comparable to the 17.0 kcal/mol for releasing N_2 from E (Figure 1), which further confirms that the preference of deprotonation over N_2 extrusion in E is due to the very facile

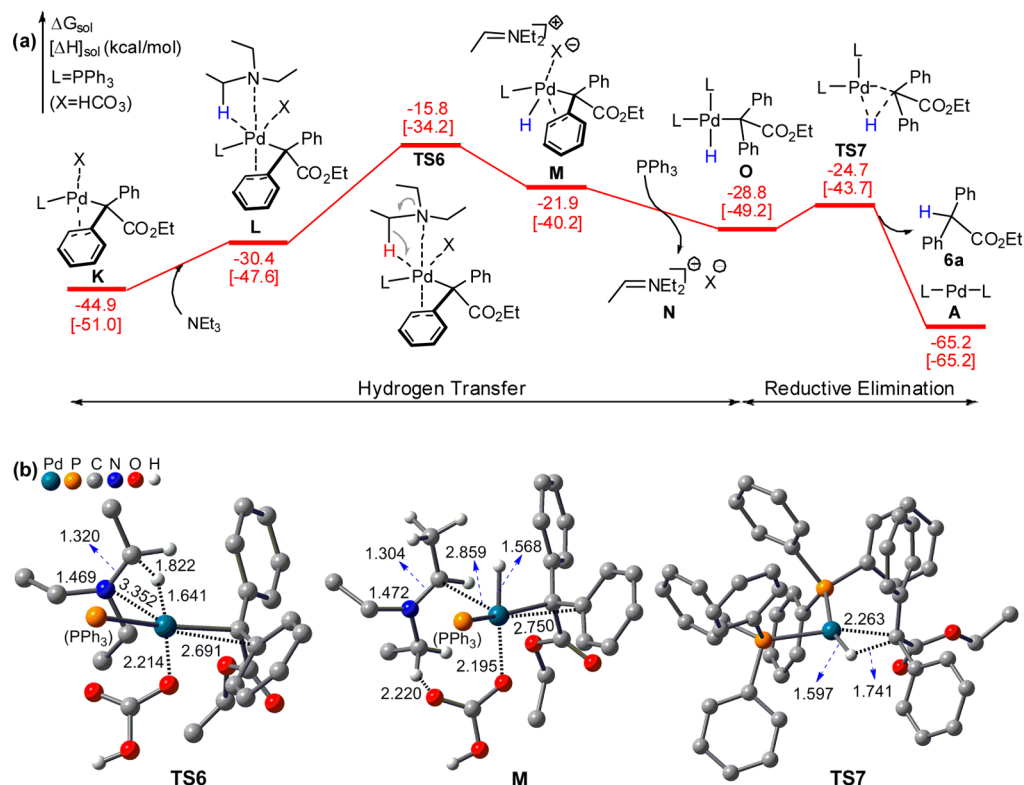


Figure 3. (a) Energy profile for the reduction of the Pd(II) species **K** by NEt_3 . (b) Key optimized structures with selected bond lengths in angstroms. Trivial hydrogen atoms are omitted for clarity.

deprotonation. The palladium species **J** is a metal carbene, as validated by comparing to the X-ray structures of well-recognized palladium carbenes,^{19,20} e.g., the experimentally captured cationic Pd–carbene shown in Figure 2b.^{19e} The computed length (1.987 Å) of the formal Pd=C double bond in **J** is shorter than that in the X-ray (2.005 Å) and the computed (2.023 Å) structures of Pd–carbene, and the Wiberg bond index of the bond (0.670) in **J** is larger than that (0.567) in Pd–carbene. Moreover, Pd–carbene and **J** have similar σ and π orbitals involved in the formal Pd=C bonds (see Supporting Information, Figure S7). Similar to the palladium carbene species we reported previously,²⁰ **J** is also unstable and can easily undergo migratory insertion by crossing a barrier (TS5) of 3.8 kcal/mol. The migratory insertion results in a much more stable complex **K** (37.7 kcal/mol lower than **J**) with a new C–C bond formed. Note that the phenyl group in **K** still coordinates to the Pd center with one of its formal C=C double bonds. Because the transformation from **J** to **K** is very feasible in terms of both kinetics and thermodynamics, it would be difficult to detect the palladium carbene species **J** experimentally. The energetic results indicate that **5a** is able to react with **H** to produce Pd–carbene species feasibly via N_2 release. However, the overall barrier for the coupling of PhI with **2a** (13.8 kcal/mol from **F** to **TS3** in Figure 1) is lower than that for dediazonation of **5a** (17.3 kcal/mol from **H** to **TS4** in Figure 2). Therefore, in coupling I stage under room temperature, the catalyst (**A**) would prefer acting on the coupling of PhI with **2a** rather than **5a**, as far as **2a** is available in the system.

The generation of **K** from **A** is highly exergonic. To produce the final product **6a** and complete the catalytic cycle, the $-\text{C}(\text{Ph})_2\text{COOEt}$ fragment needs to gain a hydrogen atom and the Pd(II) species needs to be reduced to Pd(0) complex.

Previously, NEt_3 was reported to reduce Pd(II) species,²¹ We also used NEt_3 as a reductant for the reduction of the Pd(II) species **K**. As shown in Figure 3, NEt_3 approaches the Pd(II) center of **K**, leading to complex **L**. Subsequently, a $\text{C}_\alpha\text{-H}$ atom of NEt_3 transfers to the Pd(II) center through **TS6** by crossing a barrier of 29.1 kcal/mol (relative to **K** + NEt_3), leading to **M** which contains an ion pair. After displacing the ion-pair **N** by a phosphine ligand giving **O**, reductive elimination via **TS7** takes place, resulting in the final product **6a** and regenerating the Pd(0) catalyst (**A**). The process (**K** + NEt_3 + PPh_3 → **6a** + **N** + **A**) spans a barrier of 29.1 kcal/mol and is exergonic by 20.3 kcal/mol. We realized that, considering the reaction temperature (65 °C), the barrier is somewhat high, though the value lies in the acceptable range, considering the accuracy that computational methods can reach. To corroborate the mechanism, we further examined a possible alternative that the HCO_3^- moiety in **K** offers a hydrogen atom to form **6a**, but the hydrogen transfer from HCO_3^- either to the $-\text{C}(\text{Ph})_2\text{COOEt}$ fragment or to the Pd(II) center was found to be unlikely (see Supporting Information, Figures S5 and S6).

Comparing the two coupling stages, coupling I is more favorable than coupling II. The rate-determining step for the whole transformation is the hydrogen transfer from NEt_3 to the Pd(II) species (**TS6**) in coupling II. This is in agreement with our experiments that the reaction can operate to produce **5a** (via coupling I) under room temperature, while we need to elevate the temperature (65 °C) for the tandem transformation via coupling I followed by coupling II.

CONCLUSION

We have reported herein the palladium-catalyzed C–H functionalization of acyldiazomethanes. Silver salt Ag_2CO_3

was revealed to be the optimal additive that could significantly improve the yields of the coupling products. The present reaction conditions are milder than the original ones and proved efficient over a wide range of substrates, thus providing a practical approach to introduce diazo functionality to organic compounds. Furthermore, a one-pot tandem coupling process for the synthesis of α,α -diaryl esters was developed via palladium-catalyzed cross-coupling of aryl iodides with the resulted diazo compounds. The three-component cross-coupling of EDA with two different aryl iodides could also be realized through adding the aryl iodides in separate manner.

Computational study provides interesting insights into the reaction mechanism. For the palladium-catalyzed coupling of EDA with phenyl iodide, the intriguing issue is the retention of the diazo functionality in the transformation. Computational study indicates that the dinitrogen extrusion from the Pd–EDA complex is energetically less favored as compared with the Ag_2CO_3 assisted deprotonation process by 16.8 and 11.5 kcal/mol (see Figure 1, and Figure S1 in Supporting Information) under the two deprotonation scenarios, respectively, which is in good agreement with the experimental observation. For the palladium-catalyzed coupling of diazoacetate intermediate with phenyl iodide, computational study supports the involvement of Pd–carbene as reactive intermediate, which undergoes rapid migratory insertion process with a low energy barrier of 3.8 kcal/mol. The calculation also indicates that the rate-limiting step for the overall tandem transformation is the hydrogen transfer from NEt_3 to the palladium species generated from the migratory insertion of Pd–carbene.

■ ASSOCIATED CONTENT

● Supporting Information

Experimental procedure, characterization data, copies of ^1H and ^{13}C NMR spectra, and DFT calculation details. This material is available free of charge via the Internet at <http://pubs.acs.org>.

■ AUTHOR INFORMATION

Corresponding Authors

*zxwang@ucas.ac.cn

*wangjb@pku.edu.cn

Author Contributions

[†]F.Y., S.Q., and L.Z. contributed equally to this work.

Notes

The authors declare no competing financial interest.

■ ACKNOWLEDGMENTS

The project is supported by the National Basic Research Program of China (973 Program, no. 2015CB856600) and the Natural Science Foundation of China [Grants 21472004, 21332002, and 21373216 (to Z.-X.W.)].

■ REFERENCES

(1) For selected reviews on transition-metal-catalyzed reaction of diazo compounds, see: (a) Padwa, A.; Austin, D. J. *Angew. Chem., Int. Ed. Engl.* **1994**, *33*, 1797. (b) Ye, T.; McKervy, M. A. *Chem. Rev.* **1994**, *94*, 1901. (c) Padwa, A.; Weingarten, M. D. *Chem. Rev.* **1996**, *96*, 223. (d) Doyle, M. P.; McKervy, M. A.; Ye, T. *Modern Catalytic Methods for Organic Synthesis with Diazo Compounds*; Wiley-Interscience: New York, 1998. (e) Doyle, M. P.; Forbes, D. C. *Chem. Rev.* **1998**, *98*, 911. (f) Hodgson, D. M.; Pierard, F. Y. T. M.; Stuppel, P. A. *Chem. Soc. Rev.* **2001**, *30*, 50. (g) Davies, H. M. L.; Beckwith, R. E. J. *Chem. Rev.* **2003**, *103*, 2861. (h) Gois, P. M. P.; Afonso, C. A. M. *Eur. J. Org. Chem.* **2004**, 3773. (i) Davies, H. M. L.

Nikolai, J. *Org. Biomol. Chem.* **2005**, *3*, 4176. (j) Davies, H. M. L.; Manning, J. R. *Nature* **2008**, *451*, 417. (k) Zhou, C.-Y.; Huang, J.-S.; Che, C.-M. *Synlett* **2010**, 2681. (l) Doyle, M. P.; Duffy, R.; Ratnikov, M.; Zhou, L. *Chem. Rev.* **2010**, *110*, 704. (m) Davies, H. M. L.; Morton, D. *Chem. Soc. Rev.* **2011**, *40*, 1857. (n) Davies, H. M. L.; Lian, Y. *Acc. Chem. Res.* **2012**, *45*, 923. (o) Zhu, S.-F.; Zhou, Q.-L. *Acc. Chem. Res.* **2012**, *45*, 1365. (p) Guo, X.; Hu, W. *Acc. Chem. Res.* **2013**, *46*, 2427. (q) Murphy, G. K.; Stewart, C.; West, F. G. *Tetrahedron* **2013**, *69*, 2667.

(2) Peng, C.; Cheng, J.; Wang, J. *J. Am. Chem. Soc.* **2007**, *129*, 8708.

(3) (a) Bablinski, D. J.; Aguilar, H. R.; Still, R.; Frantz, D. E. *J. Org. Chem.* **2011**, *76*, 5915. (b) Eidamshaus, C.; Hommes, P.; Reissig, H.-U. *Synlett* **2012**, 23, 1670.

(4) For selected reviews on the functionalization of C–H bonds, see: (a) Crabtree, R. H. *Chem. Rev.* **1985**, *85*, 245. (b) Beller, M.; Bolm, C. *Transition Metals for Organic Synthesis*; Wiley-VCH: Weinheim, Germany, 2004. (c) Dyker, G. *Handbook of C–H Transformations. Applications in Organic Synthesis*; Wiley-VCH: Weinheim, Germany, 2005. (d) Godula, K.; Sames, D. *Science* **2006**, *312*, 67. (e) Bergman, R. G. *Nature* **2007**, *446*, 391. (f) Giri, R.; Shi, B.-F.; Engle, K. M.; Mauge, N.; Yu, J.-Q. *Chem. Soc. Rev.* **2009**, *38*, 3242. (g) Ackermann, L.; Vicente, R.; Kapdi, A. R. *Angew. Chem., Int. Ed.* **2009**, *48*, 9792. (h) Mkhali, I. A. I.; Barnard, J. H.; Marder, T. B.; Murphy, J. M.; Hartwig, J. F. *Chem. Rev.* **2010**, *110*, 890. (i) Lyons, T. W.; Sanford, M. S. *Chem. Rev.* **2010**, *110*, 1147. (j) Jazsar, R.; Hitce, J.; Renaudat, A.; Sofack-Kreutzer, J.; Baudoin, O. *Chem.—Eur. J.* **2010**, *16*, 2654. (k) Ackermann, L. *Chem. Rev.* **2011**, *111*, 1315. (l) Yeung, C. S.; Dong, V. M. *Chem. Rev.* **2011**, *111*, 1215. (m) Arockiam, P. B.; Bruneau, C.; Dixneuf, P. H. *Chem. Rev.* **2012**, *112*, 5879. (n) Li, B.-J.; Shi, Z.-J. *Chem. Soc. Rev.* **2012**, *41*, 5588.

(5) For a recent review on the synthesis of diazo compounds, see: Maas, G. *Angew. Chem., Int. Ed.* **2009**, *48*, 8186.

(6) We have recently reported an alternative approach through Pd(0)-catalyzed deacylative cross-coupling of aryl iodides with acyldiazocarbonyl compounds, see: Ye, F.; Wang, C.; Zhang, Y.; Wang, J. *Angew. Chem., Int. Ed.* **2014**, *53*, 11625.

(7) For reviews, see: (a) Zhang, Y.; Wang, J. *Eur. J. Org. Chem.* **2011**, 1015. (b) Barluenga, J.; Valdés, C. *Angew. Chem., Int. Ed.* **2011**, *50*, 7486. (c) Shao, Z.; Zhang, H. *Chem. Soc. Rev.* **2011**, *41*, 560. (d) Xiao, Q.; Zhang, Y.; Wang, J. *Acc. Chem. Res.* **2013**, *46*, 236. (e) Xia, Y.; Zhang, Y.; Wang, J. *ACS Catal.* **2013**, *3*, 2586. (f) Liu, Z.; Wang, J. *J. Org. Chem.* **2013**, *78*, 10024.

(8) For selected examples, see: (a) Greenman, K. L.; Carter, D. S.; Van Vranken, D. L. *Tetrahedron* **2001**, *57*, 5219. (b) Barluenga, J.; Moriel, P.; Valdés, C.; Aznar, F. *Angew. Chem., Int. Ed.* **2007**, *46*, 5587. (c) Peng, C.; Wang, Y.; Wang, J. *J. Am. Chem. Soc.* **2008**, *130*, 1566. (d) Kudirka, R.; Devine, S. K. J.; Adams, C. S.; Van Vranken, D. L. *Angew. Chem., Int. Ed.* **2009**, *48*, 3677. (e) Yu, W.-Y.; Tsoi, Y.-T.; Zhou, Z.; Chan, A. S. C. *Org. Lett.* **2009**, *11*, 469. (f) Barluenga, J.; Escribano, M.; Aznar, F.; Valdés, C. *Angew. Chem., Int. Ed.* **2010**, *49*, 6856. (g) Zhao, X.; Jing, J.; Lu, K.; Zhang, Y.; Wang, J. *Chem. Commun.* **2010**, 1724. (h) Zhou, L.; Ye, F.; Zhang, Y.; Wang, J. *J. Am. Chem. Soc.* **2010**, *132*, 13590. (i) Barluenga, J.; Quiñones, N.; Cabal, M.-P.; Aznar, F.; Valdés, C. *Angew. Chem., Int. Ed.* **2011**, *50*, 2350. (j) Zhou, L.; Ye, F.; Ma, J.; Zhang, Y.; Wang, J. *Angew. Chem., Int. Ed.* **2011**, *50*, 3510. (k) Chen, Z.-S.; Duan, X.-H.; Wu, L.-Y.; Ali, S.; Ji, K.-G.; Zhou, P.-X.; Liu, X.-Y.; Liang, Y.-M. *Chem.—Eur. J.* **2011**, *17*, 6918. (l) Ojha, D. P.; Prabhu, K. R. *J. Org. Chem.* **2012**, *77*, 11027. (m) Chan, W.-W.; Lo, S.-F.; Zhou, Z.; Yu, W.-Y. *J. Am. Chem. Soc.* **2012**, *134*, 13565. (n) Roche, M.; Hamze, A.; Brion, J.-D.; Alami, M. *Org. Lett.* **2013**, *15*, 148. (o) Yadav, A. K.; Srivastava, V. P.; Yadav, L. D. S. *Chem. Commun.* **2013**, 49, 2154. (p) Yang, K.; Zhang, J.; Li, Y.; Cheng, B.; Zhao, L.; Zhai, H. *Org. Lett.* **2013**, *15*, 808. (q) Zeng, X.; Cheng, G.; Shen, J.; Cui, X. *Org. Lett.* **2013**, *15*, 3022. (r) Liu, X.; Ma, X.; Huang, Y.; Gu, Z. *Org. Lett.* **2013**, *15*, 4814. (s) Barroso, R.; Valencia, R. A.; Cabal, M.-P.; Valdés, C. *Org. Lett.* **2014**, *16*, 2264. (t) Wang, P.-S.; Lin, H.-C.; Zhou, X.-L.; Gong, L.-Z. *Org. Lett.* **2014**, *16*, 3332. (u) Zhou, P.-X.; Ye, Y.-Y.; Ma, J.-W.; Zheng, L.; Tang, Q.

Qiu, Y.-F.; Song, B.; Qiu, Z.-H.; Xu, P.-F.; Liang, Y.-M. *J. Org. Chem.* **2014**, *79*, 6627.

(9) For recent reviews on tandem catalysis, see: (a) Fogg, D. E.; dos Santos, E. N. *Coord. Chem. Rev.* **2004**, *248*, 2365. (b) Müller, T. J. J. *Top. Organomet. Chem.* **2006**, *19*, 149. (c) Shindoh, N.; Takemoto, Y.; Takasu, K. *Chem.—Eur. J.* **2009**, *15*, 12168. (d) Ajamian, A.; Gleason, J. L. *Angew. Chem., Int. Ed.* **2004**, *43*, 3754. (e) Ajamian, A.; Gleason, J. L. *Chem. Rev.* **2005**, *105*, 1001 and references therein. (f) Albrecht, L.; Jiang, H.; Jørgensen, K. A. *Angew. Chem., Int. Ed.* **2011**, *50*, 8492. (g) Grondal, C.; Jeanty, M.; Enders, D. *Nat. Chem.* **2010**, *2*, 167. (h) Vaxelaire, C.; Winter, P.; Christmann, M. *Angew. Chem., Int. Ed.* **2011**, *50*, 3605.

(10) Zhao, X.; Zhang, Y.; Wang, J. *Chem. Commun.* **2012**, *48*, 10162.

(11) (a) Yadav, J. S.; Reddy, B. V. S.; Sathesh, G. *Tetrahedron Lett.* **2003**, *44*, 833. (b) Johansen, M. B.; Kerr, M. A. *Org. Lett.* **2010**, *12*, 4956. (c) Cai, Y.; Zhu, S.-F.; Wang, G.-P.; Zhou, Q.-L. *Adv. Synth. Catal.* **2011**, *353*, 2939.

(12) (a) Lee, E. C.; Fu, G. C. *J. Am. Chem. Soc.* **2007**, *129*, 12066. (b) Hou, Z.; Wang, J.; He, P.; Wang, J.; Qin, B.; Liu, X.; Lin, L.; Feng, X. *Angew. Chem., Int. Ed.* **2010**, *49*, 4763.

(13) Frisch, M. J.; Trucks, G. W.; Schlegel, H. B.; Scuseria, G. E.; Robb, M. A.; Cheeseman, J. R.; Scalmani, G.; Barone, V.; Mennucci, B.; Petersson, G. A.; Nakatsuji, H.; Caricato, M.; Li, X.; Hratchian, H. P.; Izmaylov, A. F.; Bloino, J.; Zheng, G.; Sonnenberg, J. L.; Hada, M.; Ehara, M.; Toyota, K.; Fukuda, R.; Hasegawa, J.; Ishida, M.; Nakajima, T.; Honda, Y.; Kitao, O.; Nakai, H.; Vreven, T.; Montgomery, J. A., Jr.; Peralta, J. E.; Ogliaro, F.; Bearpark, M.; Heyd, J. J.; Brothers, E.; Kudin, K. N.; Staroverov, V. N.; Kobayashi, R.; Normand, J.; Raghavachari, K.; Rendell, A.; Burant, J. C.; Iyengar, S. S.; Tomasi, J.; Cossi, M.; Rega, N.; Millam, N. J.; Klene, M.; Knox, J. E.; Cross, J. B.; Bakken, V.; Adamo, C.; Jaramillo, J.; Gomperts, R.; Stratmann, R. E.; Yazyev, O.; Austin, A. J.; Cammi, R.; Pomelli, C.; Ochterski, J. W.; Martin, R. L.; Morokuma, K.; Zakrzewski, V. G.; Voth, G. A.; Salvador, P.; Dannenberg, J. J.; Dapprich, S.; Daniels, A. D.; Farkas, Ö.; Foresman, J. B.; Ortiz, J. V.; Cioslowski, J.; Fox, D. J. *Gaussian 09*, revision A.01; Gaussian, Inc.: Wallingford, CT, 2009.

(14) All the structures were optimized and characterized to be energy minima or transition states at M06/BSI level, where BSI denotes a basis set of LANL2DZ for Pd, I, Ag and 6-31G(d) for other atoms. The energies were then improved by M06/BSII//M06/BSI single-point calculations with the solvent effects accounted by SMD solvent model, using toluene as the solvent. BSII denotes a basis set of SDD for Pd, I, Ag and 6-311++G(d,p) for other atoms. The gas-phase M06/BSI harmonic frequencies were used for thermal corrections to free energies at 298.15 K and 1 atm. More details are given in Supporting Information.

(15) (a) Nicolaou, K. C.; Bulger, P. G.; Sarlah, D. *Angew. Chem., Int. Ed.* **2005**, *44*, 4442. (b) Beletskaya, I. P.; Cheprakov, A. V. *Chem. Rev.* **2000**, *100*, 3009. (c) Espinet, P.; Echavarren, A. M. *Angew. Chem., Int. Ed.* **2004**, *43*, 4704. (d) Chinchilla, R.; Najera, C. *Chem. Rev.* **2007**, *107*, 874. (e) Suzuki, A. *J. Organomet. Chem.* **1999**, *576*, 147.

(16) (a) Casado, A. L.; Espinet, P. *Organometallics* **1998**, *17*, 954. (b) Braga, A. A. C.; Ujaque, G.; Maseras, F. *Organometallics* **2006**, *25*, 3647.

(17) (a) Ahlquist, M.; Norrby, P. O. *Organometallics* **2007**, *26*, 550. (b) Lam, K. C.; Marder, T. B.; Lin, Z. Y. *Organometallics* **2007**, *26*, 758. (c) Surawatanawong, P.; Fan, Y.; Hall, M. B. *J. Organomet. Chem.* **2008**, *693*, 1552. (d) Ahlquist, M.; Fristrup, P.; Tanner, D.; Norrby, P. O. *Organometallics* **2006**, *25*, 2066.

(18) (a) Wiberg, K. B. *Tetrahedron* **1968**, *24*, 1083. (b) Reed, A. E.; Curtiss, L. A.; Weinhold, F. *Chem. Rev.* **1988**, *88*, 899.

(19) For reports on the structure of palladium carbene, see: (a) Taubmann, C.; Öfele, K.; Herdtweck, E.; Herrmann, W. A. *Organometallics* **2009**, *28*, 4254. (b) Taubmann, C.; Tosh, E.; Öfele, K.; Herdtweck, E.; Herrmann, W. A. *J. Organomet. Chem.* **2008**, *693*, 2231. (c) Herrmann, W. A.; Öfele, K.; Taubmann, C.; Herdtweck, E.; Hoffmann, S. D. *J. Organomet. Chem.* **2007**, *692*, 3846. (d) Schneider, S. K.; Roembke, P.; Julius, G. R.; Raubenheimer, H. G.; Herrmann, W. A. *Adv. Synth. Catal.* **2006**, *348*, 1862. (e) Schuster, O.;

Raubenheimer, H. G. *Inorg. Chem.* **2006**, *45*, 7997. (f) Oulié, P.; Nebra, N.; Saffon, N.; Maron, L.; Martin-Vaca, B.; Bourissou, D. *J. Am. Chem. Soc.* **2009**, *131*, 3493. (g) Weng, W.; Chen, C.-H.; Foxman, B. M.; Ozerov, O. V. *Organometallics* **2007**, *26*, 3315. (h) Stander-Grobler, E.; Schuster, O.; Heydenrych, G.; Cronje, S.; Tosh, E.; Albrecht, M.; Frenking, G.; Raubenheimer, H. G. *Organometallics* **2010**, *29*, 5821. (i) Kessler, F.; Szesni, N.; Pöhako, K.; Weibert, B.; Fischer, H. *Organometallics* **2009**, *28*, 348. (j) Vignolle, J.; Gornitzka, H.; Donnadiet, B.; Bourissou, D.; Bertrand, G. *Angew. Chem., Int. Ed.* **2008**, *47*, 2271.

(20) Xia, Y.; Qu, S.; Xiao, Q.; Wang, Z.-X.; Qu, P.; Chen, L.; Liu, Z.; Tian, L.; Huang, Z.; Zhang, Y.; Wang, J. *J. Am. Chem. Soc.* **2013**, *135*, 13502.

(21) (a) Negishi, E.-i., de Meijere, A. *Handbook of Organopalladium Chemistry for Organic Synthesis*; Wiley: New York, 2002. (b) Muzart, J. *J. Mol. Catal. A: Chem.* **2009**, *308*, 15. (c) Kuehne, M. E.; Hall, T. C. *J. Org. Chem.* **1976**, *41*, 2742.